DOI: 10.1039/C2CC34109C (Communication) *Chem. Commun.*, 2012, **48**, 8490-8492

J-aggregation induced low bandgap anthracene-based conjugated molecule for solution-processed solar cells†

Jicheol Shin [a], Nam Su Kang [bc], Kyung Hwan Kim [a], Tae Wan Lee [a], Jung-Il Jin [a], Minsik Kim [a], Kwangyeol Lee [a], Byeong Kwon Ju [b], Jae-Min Hong [c] and Dong Hoon Choi *[a]

[a] *Department of Chemistry, College of Science, Research Institute for Natural Sciences, Korea University, 145 Anam-ro, Seongbuk-gu, Seoul 136-713, Republic of Korea. E-mail: dhchoi8803@korea.ac.kr; Fax: +82-2-924-3141; Tel: +82-2-3290-3140*

[b] *Display and Nanosystem Laboratory, College of Engineering, Korea University, 145 Anam-ro, Seongbuk-gu, Seoul 136-713, Republic of Korea*

[c] *Future Convergence Research Division, Korea Institute of Science and Technology, P.O. Box 131, Cheongryang, Seoul 130-650, Republic of Korea*

Received 8th June 2012 , Accepted 27th June 2012

First published on the web 27th June 2012

A new anthracene-based X-shaped conjugated molecule, **HBTATHT**, was synthesized. Thin film transistors based on unannealed **HBTATHT** showed a carrier mobility of 0.15 $cm^2\ V^{-1}\ s^{-1}$ ($I_{on/off} = 7.9 \times 10^6$). Further, a solution processed solar cell made of **HBTATHT** exhibited promising power conversion efficiencies of 4.84% and 4.70% with $PC_{61}BM$ (1 : 0.8 wt ratio) and $PC_{71}BM$ (1 : 0.6 wt ratio), respectively.

Small semiconducting organic molecules are of particular interest because the synthesis/purification is easy, their electronic properties are easily fine-tuned, and the performance of the corresponding photovoltaic (PV) devices is very reproducible.[1–3] Very recently, there were very interesting serial works done by Y. Chen's group.[3] They firstly synthesized linear semiconducting molecules, which exhibited 5.08–6.1% efficiency in PV cells.[3] For high performance, the donor and acceptor materials should form nanoscale interpenetrating networks to enable an efficient exciton diffusion and dissociation process. However, [6,6]-phenyl-C61-butyric acid methyl ester ($PC_{61}BM$) shows an intrinsic ease of crystallization, leading to large-scale phase separation, which is detrimental to the performance of PV devices. In order to overcome this intrinsic limit of $PC_{61}BM$ type of molecules, diiodooctane has been used by Y. Sun *et al.* as a solvent additive to boost the PV performance to 6.7% efficiency while the PV showed solar cell efficiency around 1.06–4.52% without the additive.[4] Although there were some reports about outstanding small molecule-based OPVs as mentioned above,[3,4] herein we report another promising example of annealing-free photovoltaic paint with the long-range ordering of the individual molecules and optimized nanophase segregation occurring immediately after the spin-coating of the solution.

For a facilitated carrier transport in the bulk heterojunction (BHJ), high charge carrier mobility for both holes and electrons is essential. High molecular order and crystallinity should be sustained even after the mixing of two electronically antagonistic materials. However, the miscible blending of two components always hampers the separate formation of crystalline domains of each component and a highly immiscible blend induces the formation of large-scale crystallites with very poor mobility. In addition, the electronic bandgap of a p-type semiconducting material should be tuned to enable the increased absorption of light from the solar emission spectrum. For this purpose, low bandgap materials could be the best candidates; in order to address these issues, we designed a low bandgap p-type small molecule without electron withdrawing groups. By anchoring 5-ethynyl-5′-hexyl-2,2′-

ChemComm

Cite this: *Chem. Commun.*, 2012, **48**, 8490–8492

www.rsc.org/chemcomm

COMMUNICATION

J-aggregation induced low bandgap anthracene-based conjugated molecule for solution-processed solar cells†

Jicheol Shin,[a] Nam Su Kang,[bc] Kyung Hwan Kim,[a] Tae Wan Lee,[a] Jung-Il Jin,[a] Minsik Kim,[a] Kwangyeol Lee,[a] Byeong Kwon Ju,[b] Jae-Min Hong[c] and Dong Hoon Choi*[a]

Received 8th June 2012, Accepted 27th June 2012
DOI: 10.1039/c2cc34109c

A new anthracene-based X-shaped conjugated molecule, HBTATHT, was synthesized. Thin film transistors based on unannealed HBTATHT showed a carrier mobility of 0.15 cm^2 V^{-1} s^{-1} ($I_{on/off}$ = 7.9 × 10^6). Further, a solution processed solar cell made of HBTATHT exhibited promising power conversion efficiencies of 4.84% and 4.70% with $PC_{61}BM$ (1 : 0.8 wt ratio) and $PC_{71}BM$ (1 : 0.6 wt ratio), respectively.

Small semiconducting organic molecules are of particular interest because the synthesis/purification is easy, their electronic properties are easily fine-tuned, and the performance of the corresponding photovoltaic (PV) devices is very reproducible.[1–3] Very recently, there were very interesting serial works done by Y. Chen's group.[3] They firstly synthesized linear semiconducting molecules, which exhibited 5.08–6.1% efficiency in PV cells.[3] For high performance, the donor and acceptor materials should form nanoscale interpenetrating networks to enable an efficient exciton diffusion and dissociation process. However, [6,6]-phenyl-C61-butyric acid methyl ester ($PC_{61}BM$) shows an intrinsic ease of crystallization, leading to large-scale phase separation, which is detrimental to the performance of PV devices. In order to overcome this intrinsic limit of $PC_{61}BM$ type of molecules, diiodooctane has been used by Y. Sun *et al.* as a solvent additive to boost the PV performance to 6.7% efficiency while the PV showed solar cell efficiency around 1.06–4.52% without the additive.[4] Although there were some reports about outstanding small molecule-based OPVs as mentioned above,[3,4] herein we report another promising example of annealing-free photovoltaic paint with the long-range ordering of the individual molecules and optimized nanophase segregation occurring immediately after the spin-coating of the solution.

[a] *Department of Chemistry, College of Science, Research Institute for Natural Sciences, Korea University, 145 Anam-ro, Seongbuk-gu, Seoul 136-713, Republic of Korea. E-mail: dhchoi8803@korea.ac.kr; Fax: +82-2-924-3141; Tel: +82-2-3290-3140*
[b] *Display and Nanosystem Laboratory, College of Engineering, Korea University, 145 Anam-ro, Seongbuk-gu, Seoul 136-713, Republic of Korea*
[c] *Future Convergence Research Division, Korea Institute of Science and Technology, P.O. Box 131, Cheongryang, Seoul 130-650, Republic of Korea*

† Electronic supplementary information (ESI) available: Synthetic details, instrumentation, OFET device fabrication, thermal analysis, CV data, AFM images, XRD data *etc.* See DOI: 10.1039/c2cc34109c

For a facilitated carrier transport in the bulk heterojunction (BHJ), high charge carrier mobility for both holes and electrons is essential. High molecular order and crystallinity should be sustained even after the mixing of two electronically antagonistic materials. However, the miscible blending of two components always hampers the separate formation of crystalline domains of each component and a highly immiscible blend induces the formation of large-scale crystallites with very poor mobility. In addition, the electronic bandgap of a p-type semiconducting material should be tuned to enable the increased absorption of light from the solar emission spectrum. For this purpose, low bandgap materials could be the best candidates; in order to address these issues, we designed a low bandgap p-type small molecule without electron withdrawing groups. By anchoring 5-ethynyl-5′-hexyl-2,2′-bithiophene at the 9,10-position of the anthracene ring, we obtained a low bandgap of 1.86 eV for **HBTATHT**.

OPV cell performances are strongly dependent on the nanoscale morphology of the donor and acceptor in the solid-state of the photoactive layer. Therefore, we first examined the internal morphologies of the blend matrices before considering the corresponding PV devices. The transmission electron microscopy (TEM) images, showing obvious differences, are illustrated in Fig. 1(B)–(E). Both TEM images (B) and (D) of the blend films possess uniform and fine features, suggesting a well-defined nanoscale phase separation. The dark regions in the TEM images are attributed to PCBM-rich domains since PCBM scatters electrons more efficiently and the bright regions to the **HBTATHT**-rich domains in which small elongated crystallites (width ~2–3 nm, length ~15–30 nm) overlap with each other over the entire film. In particular, PCBM nanocrystals are elongated and randomly distributed in the blend film and large PCBM crystals could not be observed. The formation of elongated $PC_{61}BM$ nanocrystals provides an efficient percolation path for the charge carriers. In contrast, the TEM image of the blend film with a 1 : 1 wt ratio (see Fig. 1(C)) exhibits only large-scale phase separation and a less bicontinuous network structure. In an extremely poor case, large spherical $PC_{71}BM$ crystals (diameters ~100–200 nm) were observed clearly in a **HBTATHT** : $PC_{71}BM$ (1 : 2) sample. From the TEM analysis, we could optimize the composition of **HBTATHT** and PCBM for observing the most efficient nanophase segregation (Fig. 1(A)).

To elucidate the HOMO and LUMO energy levels of **HBTATHT**, its electrochemical properties were investigated

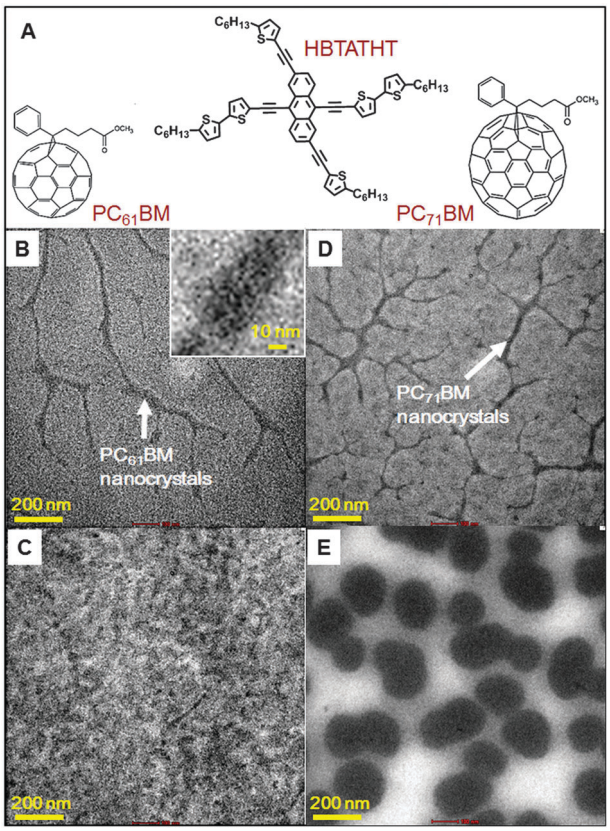

Fig. 1 (A) Structures of **HBTATHT**, $PC_{61}BM$, and $PC_{71}BM$. (B) and (C) TEM images of **HBTATHT** : $PC_{61}BM$ with 1 : 0.8 and 1 : 1 wt ratios, respectively. (D) and (E) TEM image of **HBTATHT** : $PC_{71}BM$ with 1 : 0.6 and 1 : 2 wt ratios. PCBM nanocrystals are denoted with white arrows.

by cyclic voltammetry (see Fig. S5, ESI†). Voltammograms of **HBTATHT** films show that their lowest oxidative waves are at around +1.00 V. The film has a HOMO level of −5.39 eV and a LUMO energy level of around −3.53 eV. To our knowledge, **HBTATHT** is one of the very few p-type semiconducting molecules that can display a low bandgap energy of 1.86 eV without containing electron-accepting moieties.

Fig. 2(A) shows the absorption and emission spectra of the solution, as-spun film, and thermally annealed film of **HBTATHT**. We observe a significant red shift ($\Delta\lambda$ = 108 nm) upon film formation, which indicates strong inter-molecular interactions among the molecules in the films. The absorption and emission spectra of the as-spun film of **HBTATHT** do not change significantly even after thermal annealing, and this proves that the as-spun film prepared at room temperature already possesses a fully organized molecular crystalline structure by virtue of J-aggregation, as observed in our previous work.[5,6] Due to specific aggregation, the film provides an improved spectral overlap with that of the solar spectrum. From the XRD patterns in Fig. 2(B), the crystalline nature of **HBTATHT** is evident, and a highly resolved (100) diffraction peak was observed at 2θ = 3.94° (d = 22.4 Å), which indicates that the molecules exhibit well organized intermolecular ordering. Although PCBM was blended, the diffraction peak remained unchanged, except for line broadening. In Fig. 2(C) and (D), the absorption spectra of blend samples with **HBTATHT** and PCBMs are compared with those of **HBTATHT**. By adding

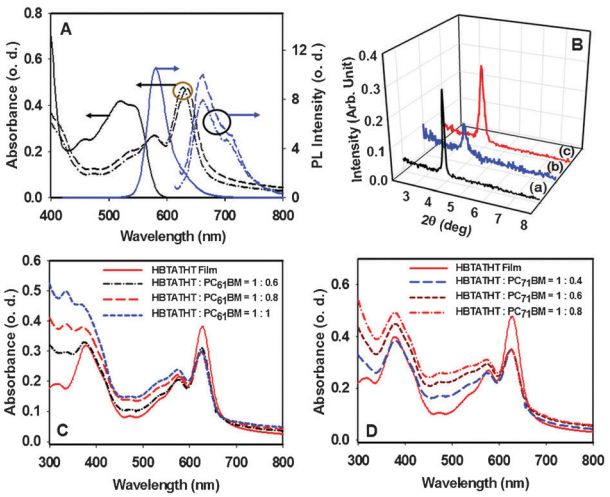

Fig. 2 (A) Absorption spectra and photoluminescence (PL) spectra of the solution (solid line), as-spun film (dashed line), and a film that is thermally annealed at 130 °C for 10 min (dash-dot-dashed line). (B) Comparison of XRD patterns. (a) **HBTATHT** pristine film, (b) **HBTATHT** : $PC_{61}BM$ = 1 : 0.8 (wt ratio), (c) **HBTATHT** : $PC_{71}BM$ = 1 : 0.6 (wt ratio). (C) Absorption spectra of **HBTATHT** and its blend films with $PC_{61}BM$. (D) Absorption spectra of **HBTATHT** and its blend films with $PC_{71}BM$.

PCBM, the absorbance at around 300–600 nm increased; however, the sharp peaks at 628 nm were highly persistent in all compositions. These results indicate that the J-aggregation-induced crystalline structure of **HBTATHT** in the blend film was robustly maintained.

Provided that PCBM molecules are appropriately positioned, nanocrystals could be formed as seen in Fig. 1(B) and (D). Efficient percolation for charge carriers between the PCBM domains is achieved by PCBM nanocrystals that fill the space between the **HBTATHT** crystalline network and form continuous channels for electron transport. The magnitude of the carrier mobility of **HBTATHT** was measured in a film state. Bottom-gate top-contact OTFT devices (L = 100 μm, W = 1500 μm) were fabricated under ambient conditions without thermal annealing. The OTFT of **HBTATHT** exhibited typical p-channel field-effect transistor (FET) characteristics. The mobilities were obtained from the source (S)–drain (D) current–drain voltage curves (I_{DS} *vs.* V_{DS}) in well-resolved saturation regions (see Fig. S8, ESI†). A sufficiently high mobility for OPV was measured, *i.e.*, 0.15 $cm^2\ V^{-1}\ s^{-1}$ ($I_{on/off}$ = 10^6–10^7). The large mobility of the device is mainly attributable to the high degree of structural order of the crystalline grains as well as the two-dimensional molecular arrangement within the grains associated with the molecular structure, having four hexyl peripheral groups. The single crystal field effect transistor (SC-FET) also exhibited high carrier mobility, *i.e.*, >0.3 $cm^2\ V^{-1}\ s^{-1}$ (see Fig. S9, ESI†).

The photovoltaic properties based on the **HBTATHT** molecule were studied in solar cells with structures of ITO/PEDOT:PSS/**HBTATHT**:$PC_{61}BM$ (or $PC_{71}BM$)/LiF/Al. The active layers were spin-coated from chlorobenzene (CB) solutions and the weight ratios of **HBTATHT** to $PC_{61}BM$ were 1 : 1, 1 : 0.8, and 1 : 0.6; the ratios of **HBTATHT** to $PC_{71}BM$ were 1 : 0.8, 1 : 0.6, and 1 : 0.4. As a control device, we fabricated a PV cell comprising a mixture of P3HT and $PC_{61}BM$ with the wt ratio of 1 : 0.6. Fig. 3(A) shows the curves of current density *versus* voltage (*J*–*V*), measured from the

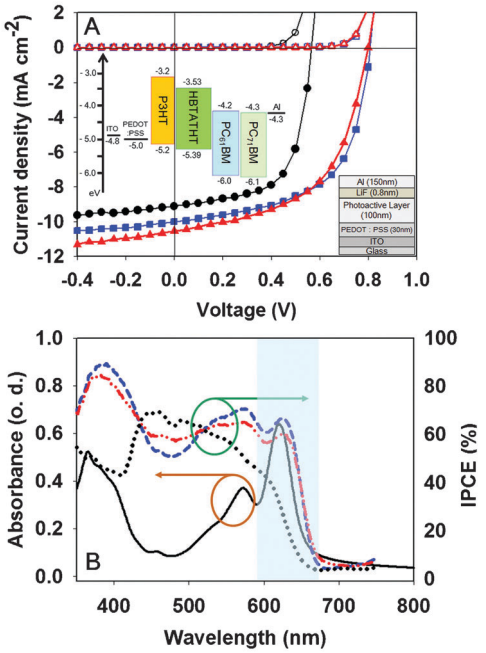

Fig. 3 (A) Current density–voltage (J–V) characteristics of OPVs based on **HBTATHT** : $PC_{61}BM$ and **HBTATHT** : $PC_{71}BM$ active layers. Open symbols: dark current, filled symbols: photocurrent. Square (1 : 0.8 ($PC_{61}BM$)), triangle (1 : 0.6 ($PC_{71}BM$)), circle (P3HT : $PC_{61}BM$ = 1 : 0.6), (B) External quantum efficiency (EQE) of OPV cells. Medium dashed line (1 : 0.8 ($PC_{61}BM$)), Dash-dot-dot-dashed line (1 : 0.6 ($PC_{71}BM$)), dotted line (P3HT : $PC_{61}BM$ = 1 : 0.6). The absorption spectrum (solid line) of **HBTATHT** film is superimposed. The shaded area denotes enhancement of absorption and EQE due to J-aggregation of **HBTATHT**.

Table 1 Photovoltaic properties of **HBTATHT** : PCBM solar cells

HBTATHT : PCBM wt ratio	J_{sc} (mA cm^{-2})	V_{oc} (V)	FF	PCE (%)	EQE (%) (λ = 575 nm/ 625 nm)
1 : 1[a]	−8.91	0.79	0.54	3.85	61.5/52.4
1 : 0.8[a]	−10.00	0.81	0.59	4.84	70.6/66.6
1 : 0.6[a]	−9.83	0.81	0.55	4.43	65.7/63.9
1 : 0.8[b]	−10.15	0.79	0.57	4.63	63.5/58.4
1 : 0.6[b]	−10.59	0.80	0.55	4.70	65.0/60.4
1 : 0.4[b]	−10.31	0.79	0.50	4.12	63.4/59.8
1 : 0.6[c]	−9.20	0.57	0.64	3.39	69.0[d]

[a] Acceptor, $PC_{61}BM$. [b] Acceptor, $PC_{71}BM$. [c] P3HT:$PC_{61}BM$. [d] λ = 452 nm.

blend samples of **HBTATHT** and PCBM under the AM 1.5 condition at 100 mW cm^{-2}. The open circuit voltage (V_{oc}) is governed by the molecular energetic relationship between **HBTATHT** and the $PC_{61}BM$ (or $PC_{71}BM$) acceptor. It is interesting to note that **HBTATHT** has a lower lying HOMO energy level (E_{HOMO} = −5.39 eV) giving rise to an increase in V_{oc} compared to the HOMO level of P3HT (see the inset of Fig. 3(A)). Among the devices prepared using CB as the processing solvent, the best performance with $PC_{61}BM$ was obtained at a weight ratio of 1 : 0.8, with V_{oc} = 0.81 V, J_{sc} = 10.00 mA cm^{-2}, a fill factor (FF) of 0.59, and an overall PCE of ~4.84%. As can be seen in Fig. 1(B), the resulting interpenetrating networks composed of **HBTATHT** crystals and aggregated nanocrystalline PCBM domains provide continuous channels for efficient hole and electron transport.

Another intriguing feature of the best performing **HBTATHT**-based PV cell is that it exhibited a maximum EQE of 70.6% and 66.6% at 575 and 625 nm, respectively, owing to a broad photoresponsive range from 350 to 690 nm, which is attributed to the formation of J-aggregates in the **HBTATHT** crystals.

In Table 1, **HBTATHT** : $PC_{71}BM$ (1 : 0.6) is listed to have a PCE of 4.70% and a comparable EQE distribution to that of $PC_{61}BM$-composites in the measured wavelength range. These results illustrate that the two different PCBM aggregates might be able to fit well in the spaces between **HBTATHT** molecules in the crystals and that this does not hamper the individual crystalline structure. Due to the small sized nanophase domain, photogenerated excitons efficiently diffuse and are separated in the blend films of **HBTATHT** : $PC_{61}BM$ (1 : 0.8) and **HBTATHT** : $PC_{71}BM$ (1 : 0.6), after reaching the interfaces of the donor and acceptor, resulting in enhanced charge carrier generation and a concomitant increase in the photocurrent.

In conclusion, we prepared a novel low bandgap p-type semiconducting molecule, **HBTATHT** without employing an electron-accepting moiety for PV device fabrication. The material exhibited high carrier mobilities of 0.15 cm^2 V^{-1} s^{-1} ($I_{on/off}$ = 7.9 × 10^6) in TFT and 0.3 cm^2 V^{-1} s^{-1} ($I_{on/off}$ = 1.5 × 10^3) in SC-FET. In particular, solution processed solar cells were successfully fabricated using **HBTATHT** and $PC_{61}BM$ (and $PC_{71}BM$). Small-molecule based OPVs showed promising power conversion efficiencies of 4.84% and 4.70% with $PC_{61}BM$ (1 : 0.8 wt ratio) and $PC_{71}BM$ (1 : 0.6 wt ratio).

This research was supported by National Research Foundation of Korea (NRF2012008797 & NRF-PRC20120005860). This work was also supported by the Korea Institute of Energy Technology Evaluation and planning (KETEP) grant funded by the Ministry of Knowledge Economy under contract No. 20103020010010-12-2-400.

Notes and references

1 (*a*) J.-H. Huang, M. Velusamy, K.-C. Ho, J.-T. Lin and C.-W. Chu, *J. Mater. Chem.*, 2010, **20**, 2820; (*b*) Y. Shu, Y.-F. Lim, Z. Li, B. Purushothaman, R. Hallani, J. E. Kim, S. R. Parkin, G. G. Malliaras and J. E. Anthony, *Chem. Sci.*, 2011, **2**, 363; (*c*) P. Dutta, W. Yang, S. H. Eom, W.-H. Lee, I. N. Kang and S.-H. Lee, *Chem. Commun.*, 2012, **48**, 573.

2 (*a*) K. Niimi, H. Mori, E. Miyazaki, I. Osaka, H. Kakizoe, K. Takimiya and C. Adachi, *Chem. Commun.*, 2012, **48**, 5892; (*b*) Q. Liu, K. Jiang, B. Guan, Z. Tang, J. Peib and Y. Song, *Chem. Commun.*, 2011, **47**, 740.

3 (*a*) Y. Liu, X. Wan, F. Wang, J. Zhou, G. Long, J. Tian, J. You, Y. Yang and Y. Chen, *Adv. Energy Mater.*, 2011, **1**, 771; (*b*) J. Zhou, X. Wan, Y. Liu, G. Long, F. Wang, Z. Li, Y. Zuo, C. Li and Y. Chen, *Chem. Mater.*, 2011, **23**, 4666; (*c*) Z. Li, G. He, X. Wan, Y. Liu, J. Zhou, G. Long, Y. Zuo, M. Zhang and Y. Chen, *Adv. Energy Mater.*, 2011, **2**, 74; (*d*) Y. Liu, X. Wan, F. Wang, J. Zhou, G. Long, J. Tian and Y. Chen, *Adv. Mater.*, 2011, **23**, 5387.

4 Y. Sun, G. C. Welch, W. L. Leong, C. J. Takacs, G. C. Bazan and A. J. Heeger, *Nat. Mater.*, 2011, **11**, 44.

5 J. A. Hur, S. Y. Bae, K. H. Kim, T. W. Lee, M. J. Cho and D. H. Choi, *Org. Lett.*, 2011, **13**, 1948.

6 K. H. Kim, S. Y. Bae, Y. S. Kim, J. A. Hur, M. H. Hoang, T. W. Lee, M. J. Cho, Y. Kim, M. Kim, J.-I. Jin, S.-J. Kim, K. Lee, S. J. Lee and D. H. Choi, *Adv. Mater.*, 2011, **23**, 3095.

